MD Simulations of Mistic: Conformational Stability in Detergent Micelles and Water†

Emi Psachoulia, Peter J. Bond, and Mark S. P. Sansom*

Department of Biochemistry, University of Oxford, South Parks Road, Oxford OX1 3QU, U.K.

Received May 4, 2006; Revised Manuscript Received May 29, 2006

ABSTRACT: Mistic is an unusual membrane protein from *Bacillus subtilis*. It appears to fold and insert autonomously into a lipid bilayer and has been suggested as a tool that aids the targeting of eukaryotic membrane proteins to bacterial membranes. The NMR structure of Mistic in detergent (LDAO) micelles has revealed it to be a four α-helix bundle. From a structural perspective, Mistic does not resemble other membrane proteins. Its external surface is not very hydrophobic, and standard methods do not predict any of its helices to be in the transmembrane orientation. Molecular dynamics simulations (simulation times ∼30 ns) in water and in detergent micelles have been used to explore the conformational stability of Mistic as a function of its environment. In water, the protein is stable, exhibiting no significant change in fold on a 30 ns time scale. In contrast, in three simulations in detergent micelles, the partial unfolding of Mistic occurred, whereby the H4 helix drifted away from the H1−H3 core. This was due to the penetration of detergent molecules between H4 and the remainder of the protein. This is unlike the behavior of several other membrane proteins, both α-helix bundles and *β*-barrels, in comparable detergent micelle simulations. The unfolding of H4 from the H1−H3 core of Mistic could be partially reversed by a simulation in which the detergent molecules were removed, and the unfolded protein was simulated in water. These results suggest that Mistic may not be a stable integrated membrane protein but rather that it may undergo a conformational change upon interaction with a membrane or membrane-like environment.

Mistic is an acronym for membrane integrating sequence for translation of integral membrane protein constructs. It is a small *Bacilus subtilis* encoded protein (hypothetical protein BSU31320) of molecular weight 13, containing 110 amino acids. It is an unusual protein because it folds and inserts into the lipid bilayer independent of the translocon machinery that is generally used to insert proteins into membranes (*1*−*4*). It has been suggested that Mistic may prove to be a useful tool that aids the targeting of eukaryotic membrane proteins to the bacterial membrane, enabling the overexpression of the latter as Mistic fusion proteins (*5*). Because it is generally difficult to overproduce eukaryotic membrane proteins in bacterial cell membranes (*6*), this may have useful implications, for example, in membrane protein structural biology.

The structure of Mistic (pdb id 1YGM) has been determined by solution phase NMR, combined with long-range restraints derived from an analysis of paramagnetic perturbation of TROSY spectra from five site-specific spin-labels (*5*). In these experiments, the protein was solublised using LDAO[1] (lauryl dimethylamine oxide), a detergent commonly used in studies of integral membrane proteins (*7*). Under these conditions, Mistic is a compact four α-helix bundle (Figure 1A). The second helix (H2) contains a central kink.

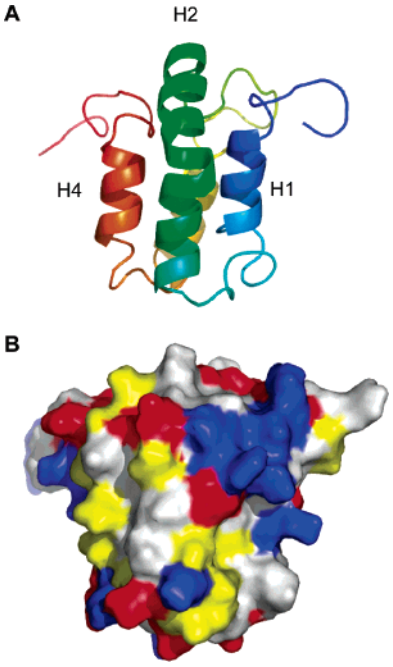

FIGURE 1: NMR structure of Mistic. (A) The fold shown in ribbon format, colored from the *N*-terminus (blue) to the *C*-terminus (red). (B) Solvent accessible surface representation, with residues colored as follows: blue = basic, red = acidic, yellow = polar, and white = hydrophobic.

Mistic has been suggested to be able to spontaneously insert into membranes. However, the surface residue distribution of Mistic (Figure 1B) is unlike that of a typical integral membrane protein (*8*) and, in particular, is unexpectedly

† This work was supported by grants from BBSRC and the Wellcome Trust.

* To whom correspondence should be addressed. Phone: 44-1865-275371. Fax: 44-1865-275273. E-mail: mark.sansom@bioch.ox.ac.uk.

[1] Abbreviations: LDAO, lauryl dimethylamine oxide; MD, molecular dynamics; RMSD, root-mean-square deviation; RMSF, root-mean-square fluctuation.

10.1021/bi0608818 CCC: $33.50
Published on Web 07/07/2006

hydrophilic. An analysis of the sequence of Mistic using a panel of 13 prediction methods (*9*) failed to predict any of the helices of Mistic as likely to adopt a transmembrane orientation. It is therefore of some interest to explore the conformational dynamics of Mistic in an aqueous and detergent micelle (i.e., a membrane mimetic) environments because this may provide some clues as to how Mistic could interact with a membrane. Extended (multinanosecond) molecular dynamics (MD) simulations (*10*, *11*) provide a computational approach to exploring membrane protein dynamics (*12*). In particular, such methods have been used to compare the conformational dynamics of membrane proteins in detergent micelle and lipid bilayer environments (*13*, *14*) and to explore the mechanisms of the self-assembly of protein/detergent micelles (*15*, *16*).

In this article, we present MD simulations of Mistic that enable us to compare its conformational stability and dynamic behavior in aqueous and detergent micelle environments. The results suggest that although Mistic is relatively stable in an aqueous environment, in the presence of a detergent, the packing of the helices (especially H4) is loosened. This is suggestive of a mechanism for membrane integration that involves helix unpacking and insertion.

METHODS

Simulation Methods. The GROMACS 3.0 simulation package (www.gromacs.org) (*17*) was used for all simulations, with a united atom version of the GROMOS96 force field (*18*) and the SPC water model (*19*). Periodic boundary conditions were applied to the systems. Long-range electrostatics were calculated using PME (*20*, *21*) with a real-space cutoff of 1 nm. A cutoff of 1 nm was used for the van der Waals interactions. All simulations were performed at a constant temperature of 300 K using the Berendsen thermostat (*22*) with a coupling constant of $\tau_T = 0.1$ ps, at a constant pressure of 1 bar using the Berendsen barostat with an isotropic coupling constant of $\tau_P = 1.0$ ps and compressibility $= 4.5 \times 10^{-5}$ bar^{-1}. The integration time step for all simulations was 2 fs, and the LINCS method (*23*) was used to constrain bond lengths. The coordinates were saved every 5 ps for analysis. An analysis of all simulations was performed using the GROMACS package. Secondary structure analysis used DSSP (*24*), and visualization and graphics used VMD (*25*) and PyMol (www.pymol.org).

Mistic Structure. The most representative conformer of the ensemble of 10 lowest energy structures in the PDB entry 1YGM was used as the starting structure for the simulations. Six residues missing from the *N*-terminus (namely, Gly-Ser-His-Gly-Met-Phe) were added using MODELLER 6v2 (http://salilab.org/modeller/modeller.html) (*26*), thus yielding the 118 residue construct employed in the structural studies. It was assumed that all ionisable residues would be in their standard charge state at neutral pH, yielding a net charge of $-11e$. This assumption was supported by pK_A calculations using PROPKA (*27*) (http://propka.chem.uiowa.edu). The protein structure was energy minimized using 100 steps of steepest descent prior to simulation setup.

LDAO. Ab initio calculations were performed to obtain partial charges for LDAO, using the program Spartan (http://www.wavefun.com/products/spartan.html) and a Hartree−Fock model with a 6-31G* basis set, singlet multiplicity, and neutral total charge. The topology of LDAO for Gromacs was obtained using PRODRG (*28*) (http://davapc1.bioch.dundee.ac.uk/programs/prodrg/). Following energy minimization, the LDAO model structure was tested via a 2 ns simulation in water. During this simulation, the LDAO molecule showed no stereochemical distortions.

Table 1: Summary of Simulations

simulation name	system setup	duration (ns)	Cα RMSD[a] (nm)
WAT	Mistic + water	30	0.6
MIC	Mistic + 50 LDAOs in a preformed micelle	30	1.2
MICSA50	Mistic + 50 LDAOs	30	0.9
MICSA78	Mistic + 78 LDAOs	20	0.7
MICWAT	30 ns structure of Mistic from the MIC simulation	10	0.9

[a] This is the value of the Cα RMSD (all residues) over the final 5 ns of each simulation.

To test the behavior of LDAO in micelle simulations, two 10 ns simulations were set up with 78 LDAO detergents (approximately equal to the aggregation number of LDAO (*29*)). One simulation was of an idealized preformed micelle, and the other simulation generated a micelle via a self-assembly micelle. Similar approaches have been used to simulate micelles of dodecyl phoshocholine (*30*) and of octyl glucoside (*31*, *32*). Both of these simulations indicated that LDAO can form a stable micelle within this time scale. The overall shape and the size of the preformed micelle did not change significantly during the 10 ns period. In the self-assembly simulation, the LDAO molecules initially formed small micelles that subsequently fused into a large micelle over the first ∼5 ns. After ∼6 ns, both systems appeared to have reached equilibrium and both micelles of similar shape and size. Combined with earlier comparisons of preformed (*13*) and self-assembled (*15*) protein/detergent micelles, the control simulations suggest that the preformed micelle and/or the self-assembly methodology may be used to study Mistic.

Simulation Systems. Five simulations of Mistic were performed (Table 1) to explore its conformational dynamics in water and a detergent (LDAO) micelle environment, the latter corresponding to the conditions under which the NMR structure was determined.

Simulation WAT (Table 1) was of Mistic in water. The protein model was solvated with 6163 SPC water molecules, and 11 sodium ions were added at random locations within the simulation box (of dimensions $7.6 \times 5.5 \times 4.6$ nm^3) to neutralize the protein charge. The resultant system (containing 18483 atoms) was then energy minimized, and the simulation run for 30 ns.

Simulation MIC was of Mistic embedded in a preformed LDAO micelle. The latter was generated as described in a previous article (*13*, *14*) using 50 LDAO molecules. This corresponds to the number of the LDAO molecules believed to be present in the protein/detergent micelles used in the NMR study (*5*). The Mistic/LDAO micelle was solvated with 9958 water molecules, and 11 Na^+ ions were added, yielding a total system of 29841 atoms, with a Na^+ ion concentration of ∼50 mM. The system was energy minimized (100 steps of steepest descent). Positional restraints were applied to the protein (to all of the nonhydrogen atoms, with a force

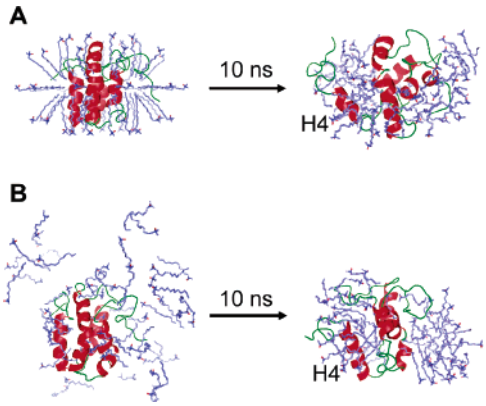

FIGURE 2: Simulation setup for two simulations of Mistic in the presence of the detergent LDAO. In each case, the left-hand image shows the system (only the protein and detergent are shown) at the start of the simulation, and the right-hand image shows the same system after 10 ns. The protein fold is shown in red ribbon format. The detergent molecules are shown either as (A) a preformed idealized micelle (simulation MIC) or (B) as detergents placed randomly around the protein molecule (simulation MICSA50).

constant of 1000 kJ mol^{-1} nm^{-1}) and a 1 ns simulation run to enable the detergent and water molecules to relax around the protein. All restraints were then removed, and the simulation ran for 30 ns.

Two simulations were performed to self-assemble Mistic/LDAO micelles, both starting with Mistic in a box (7.1 × 7.1 × 6.9 nm^3) of either 50 or 78 randomly positioned detergent molecules. The latter corresponds to the aggregation number of LDAO micelles. Both systems were solvated with ~9800 water molecules and 11 Na^+ ions. Following energy minimization, simulations of 30 ns (MICSA50) and 20 ns (MICSA78) duration were performed (Table 1).

A fifth simulation, MICWAT, was performed to explore the possible refolding (see below) of Mistic. The structure of the protein at the end of the Mic simulation (30 ns) was extracted from the micelle and placed in a box of 7543 water molecules. The resultant system was energy minimized, and a 10 ns simulation was performed.

RESULTS

The simulations performed are summarized in Table 1, where the final Cα RMSD is reported as an overall measure of the drift in conformation from the initial structure of Mistic. The RMSDs are quite high for all four simulations starting from the NMR structure, possibly reflecting the general conformational lability of this protein. However, it is evident that the degree of conformational drift in the aqueous environment (simulation WAT) is significantly less than in the presence of detergents, an aspect of the behavior of Mistic explored in more detail below.

Two classes of micelle simulation, preformed and self-assembly, were performed. These are compared visually in Figure 2. From this, it is evident that in both cases, within 10 ns the LDAO molecules have formed an irregular toroidal (i.e., doughnut-shaped) micelle around the protein molecule and that the interaction between the H4 helix and the remainder of the protein seems to have weakened. Although only the MICSA50 self-assembled simulation is shown, the same qualitative behavior was observed for the MICSA78 simulation.

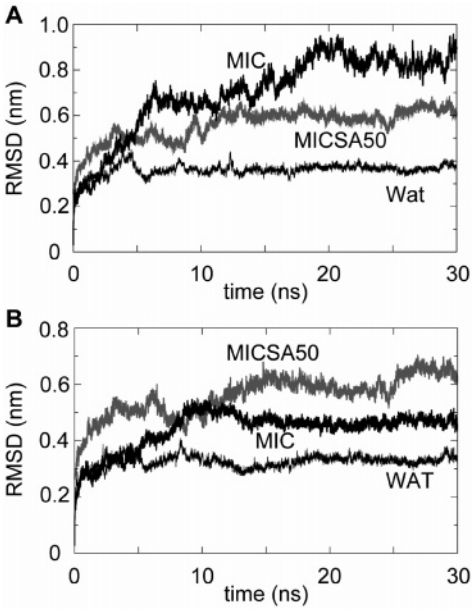

FIGURE 3: Conformational drift as measured via Cα RMSDs. (A) Cα RMSDs as a function of time for all those residues that form the four helices (i.e., residues 17−25, 37−59, 72−86, and 91−105) in the initial structure, for the WAT (thin black line), MIC (thick black line), and MICSA50 (thick gray line) simulations. (B) Cα RMSDs for those residues that form helices H1, H2, and H3 in the initial structure for the WAT (thin black line), MIC (thick black line), and MICSA50 (thick gray line) simulations.

A more quantitative measure of the degree of conformational drift of Mistic in the various simulations is provided by an evaluation of the Cα RMSD of the protein from its initial structure as a function of time. In this analysis (Figure 3A), we have omitted the consideration of the nonhelical (i.e., loop) regions because these are inherently more mobile in the majority of simulations. For the aqueous simulations (WAT), this rises to ~0.35 nm at the end of the simulation. This is comparable to that seen in simulations based on the NMR structure of the simple β-barrel membrane protein OmpA (Cox and Sansom, submitted for publication) or on the 3.5 Å resolution X-ray structure of the α-helical membrane protein LacY (Holyoake and Sansom, unpublished observations) and, thus, indicates that the structure of Mistic is broadly stable in water, at least on a 30 ns time scale.

The degree of conformation drift is surprisingly high for the simulations of Mistic in a micelle environment, given the fact that the NMR structure of the protein was determined in this environment. Thus, the Cα RMSDs for all four helices together range from ~0.6 to ~0.9 nm. This is much higher than that observed in simulations of membrane proteins in detergent micelles, with values of ~0.1 nm for the transmembrane β-barrel of OmpA (*13*) and ~0.15 nm for the transmembrane α-helix bundle of GlpF (*14*). Thus, we may conclude that Mistic undergoes substantial conformational drift in all of the simulations in the presence of a detergent.

From the initial visual inspection of the simulation (see above), it appeared that the final helix (H4) moved relative to the other helices over the course of the simulations. We, therefore, evaluated the degree of conformational drift excluding H4, by calculating the Cα RMSD versus time for the core structure formed by the H1−H3 helices (Figure 3B). For the WAT simulation, this made little difference. However, for the MIC and MICSA50 simulations, it is evident

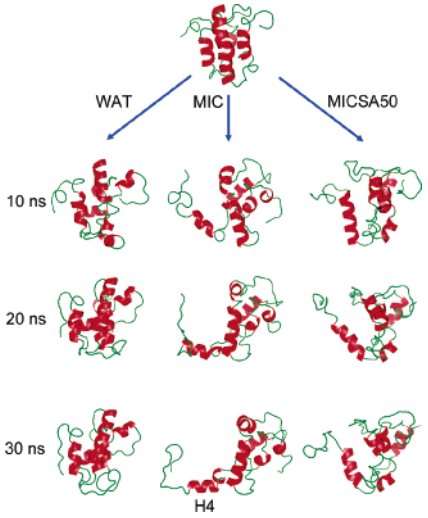

FIGURE 4: Snapshots at 10, 20, and 30 ns from the WAT, MIC, and MICSA50 simulations, showing just the protein colored on the secondary structure (red = α-helix).

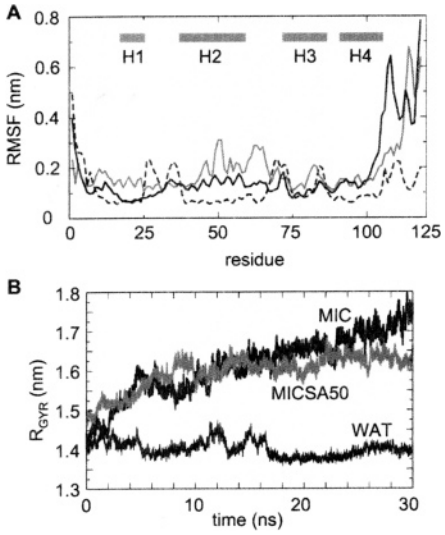

FIGURE 5: (A) Root-mean-square fluctuation (RMSF) vs residue number for the WAT (broken black line), MIC (solid black line), and MICSA50 (solid gray line) simulations. In each case, the RMSF of the Cα atoms of each residue was calculated from 17 ns until 30 ns. The reference frame was the initial model of Mistic used to set up the simulations. (B) Radius of gyration of the protein as a function of time for the WAT (thin black line), MIC (thick black line), and MICSA50 (thick gray line) simulations.

that the degree of conformational drift is less for the H1−H3 core than for the four α-helix bundle core. The behavior of the protein secondary structure (determined using DSSP (*24*)) as a function of time was analyzed (Figure S1 in Supporting Information). All four α-helices proved to be stable in the WAT simulation. Helices H2 and H3 were somewhat less stable in MICSA50, but their secondary structure was preserved in MIC. In particular, the H4 region remained α-helical in all of the simulations. Thus, the conformational drift is largely a result of changes in α-helix packing rather than the unfolding of the α-helices.

In all of the micelle simulations, a visual inspection (Figure 4) of the protein suggested that it underwent partial unfolding. In particular, helix H4 undergoes significant movements relative to those of the three other helices such that by the end of the MIC simulation, it is at a ∼90° angle to the H1−H3 helix bundle. This suggests that H4 may play a possible functional role in the interaction of Mistic with membranes (see below). Furthermore, the detergent molecules did not seem to surround all helices equally and uniformly. In contrast, in the WAT simulation, although some local loss of secondary structure seems to occur, the four helix bundle remains largely intact.

It is also of interest to examine the dynamic flexibility of Mistic as a function of the environment. To do this, the root-mean-square fluctuation (RMSF) of the Cα atoms of each residue was calculated for the latter half of the simulation (from 17 ns until 30 ns; Figure 5A). In those simulations performed in the presence of detergent, the RMSF values are generally higher than the corresponding values in the WAT simulation. In particular, the fluctuations are very high (>0.3 nm) for the latter part of H4 and the *C*-terminus of the protein. In contrast, the fluctuations for WAT are lower overall and show the expected pattern for a helix bundle, with low RMSFs for residues in the α-helices and higher values for residues in the loops. Indeed, a comparison of the mean square Cα fluctuations, averaged across all residues as a function of time (see ref 13 for details (*13*)), suggests that overall the fluctuations in the MIC and MICSA50 simulations are about 1.5 times higher than that in the WAT simulation.

The partial unfolding of Mistic in the simulations in the presence of detergents can be readily quantified by a calculation of the radius of gyration of the protein during the simulations (Figure 5B). It can be seen that the radius of gyration of Mistic in the WAT simulation is stable at 1.4 ± 0.02 nm. In contrast, in the two micelle simulations (i.e., MIC and MICSA50), the radius of gyration of the protein rises steadily over the course of the simulation, reaching ∼1.75 and ∼1.65 nm, respectively. This is clearly indicative of a degree of unfolding of the protein in the presence of a detergent. If we restrict the analysis of the radius of gyration to just helices H1−H3 (data not shown), then this value is constant with respect to time (at ∼1.2 nm for WAT, ∼1.2 nm for MIC, and ∼1.4 nm for MICSA50). This also implicates a change in the packing of H4 against H1−H3 in the unfolding process in the presence of a detergent.

We now turn our attention to the interactions of Mistic with the detergent (LDAO) molecules during the course of the micelle simulations. These interactions may be quantified as the number of contacts between protein and LDAO for which the interatomic distance is less than 0.4 nm (Figure 6). For both MIC and MICSA50 simulations, there is a steep increase in the number of protein/detergent contacts over the first ∼5 ns of the simulation. A visualization of the simulations (Figure 7) suggests that this corresponds to the initial penetration of the detergent between helix H4 and the H1−H3 core. Following this, the number of contacts fluctuates over the remainder of each simulation. In the MICSA78 simulation, the number of contacts between the detergent and Mistic (data not shown) was higher than that for the other two simulations, reflecting the larger number of detergents in the simulation box.

For all of the simulations, the numbers of the hydrogen bonds between Mistic and water were calculated (data not shown) as a function of time. In the WAT simulation, the total number of H bonds to water was constant throughout the simulation at 296 ± 14. For the detergent micelle

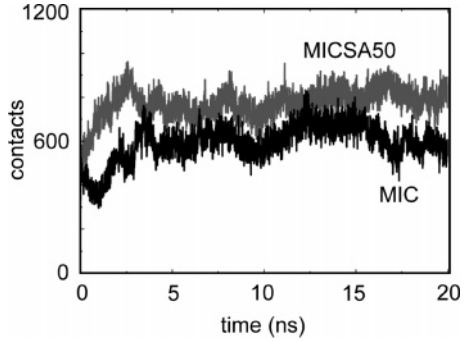

FIGURE 6: Interatomic contacts between Mistic and LDAO. The number of contacts (cutoff distance 0.4 nm) is shown as a function of time for simulations MIC (black line) and MICSA50 (grey line) over the first 20 ns of each simulation.

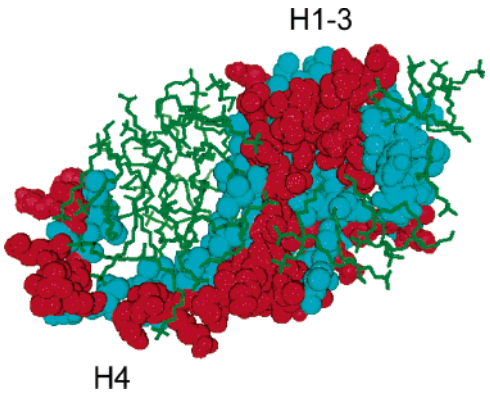

FIGURE 7: Snapshot of the MIC simulation at 30 ns, showing the protein surface (cyan = hydrophobic, red = hydrophilic) and the detergent molecules (green).

simulations (MIC and MICSA50), there was a small decrease in the number of protein/water H -bonds, from ~300 at the start of the simulation to ~260 at the end of the simulation. This decrease in protein/water H bonds mirrors the increase in protein/detergent contacts in these simulations.

To explore whether the unfolding of helix H4 from Mistic in the presence of the detergent was reversible, the protein structure from the MIC simulation at 30 ns (see Figure 4) in which H4 has completely unpacked from the H1−H3 bundle was taken and used as the starting point for a refolding simulation (MICWAT, see Table 1) in water. After ~6 ns of simulation time, the protein has refolded to the extent that the radius of gyration has fallen from ~1.75 nm back to ~1.45 nm, reaching ~1.40 nm at 9ns (Figure 8). Note that the radius of gyration of Mistic in the WAT simulation is ~1.4 nm. This partial reversal confirms that the unfolding of H4 from Mistic is due to the interactions with LDAO molecules.

DISCUSSION

In this study, we report extensive atomistic MD simulations (a total simulation time in excess of 0.1 μs) of Mistic in both detergent micelle and aqueous environments. The detergent micelle environment was chosen to match that used in the NMR studies of the protein. The results of these simulations suggest that Mistic is relatively unstable in a micellar environment and undergoes a degree of unfolding. In particular, H4 appears to unpack from H1−H3, mainly as a result of the penetration of detergent molecules between H4 and the remainder of the protein (Figure 7). This appears

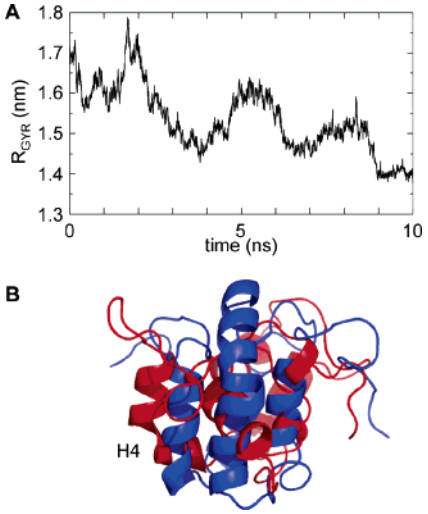

FIGURE 8: Progress of the MICWAT simulation, in which the Mistic structure from the final frame of the MIC simulation was simulated in water without any detergent present. (A) Radius of gyration of the protein as a function of time. (B) Superimposed Mistic structures at the start of the MIC (blue) and end (red) of the MICWAT simulation.

to be at least in part reversible if the detergent is then removed from the simulation system. In contrast, when simulated in an aqueous environment (i.e., in the absence of any detergent), the NMR structure of Mistic appears to be conformationally stable, at least on a time scale of tens of nanoseconds. The high flexibility and partial unfolding of Mistic in simulations in the presence of detergents is not characteristic of an integral membrane protein. Thus, the simulations of a number of membrane proteins, ranging from simple α-helix dimers (e.g., glycophorin (*15*, *33*)) and simple bacterial outer membrane proteins (e.g., OmpA (*15*) and OmpX (*34*)) through more complex α-helix bundles (e.g., GlpF (*14*)), reveal them to be stable in a detergent micelle environment on a time scale of ~10 to ~100 ns.

This instability of Mistic in a detergent micelle environment is interesting, given the suggestion that Mistic is a membrane-integrating protein. It suggests that perhaps the protein may change conformation upon its interaction with a membrane. Helix H4 is the most mobile of the helices in the detergent simulations and moves significantly relative to that of the other helices, suggesting a possible functional role in the insertion of Mistic into membranes. It is worth noting that a number of water soluble secreted proteins (e.g. δ-endotoxin (*35*), colicins (*36*)) contain α-helical domains that refold/insert upon interaction with lipid bilayers.

Of course, there are limitations to the simulations studies. Perhaps the major one is the time scale. It would be of considerable interest to simulate the interactions of Mistic with a lipid bilayer to observe any changes in H4 and possible modes of insertion. However, we would anticipate that such changes would be slow and would require a longer time scale (i.e., >100 ns) than that readily addressable by atomistic simulations. It is possible that coarse-grained simulations, which allow one to access more extended (i.e., ~1 μs) time scales, could be used to address the membrane insertion process (*37*), especially because coarse-grained methods have been used to simulate aspects of membrane/protein self-assembly (*38*). A further aspect of the simulations that may influence the details of the results is the force-

field and simulation protocol employed. For example, the treatment of long range electrostatic interactions has been shown to have some effects on protein stability in simulations (*39*, *40*).

In summary, it is clear that the mode of action of Mistic merits further examination from both an experimental and computational perspective.

ACKNOWLEDGMENT

Our thanks to all of our colleagues for their interest in this work.

SUPPORTING INFORMATION AVAILABLE

An evaluation of the secondary structure of Mistic as a function of time with DSSP. This material is available free of charge via the Internet at htttp://pubs.acs.org.

REFERENCES

1. van den Berg, B., Clemons, W. M., Collinson, I., Modis, Y., Hartmann, E., Harrison, S. C., and Rapoport, T. A. (2003) X-ray structure of a protein-conducting channel, *Nature 427*, 36−44.
2. Gorlich, D., Hartmann, E., Prehn, S., and Rapoport, T. A. (1992) A protein of the endoplasmic reticulum involved early in polypeptide translocation, *Nature 357*, 47−52.
3. Gorlich, D., Prehn, S., Hartmann, E., Kalies, K. U., and Rapoport, T. A. (1992) A mammalian homolog of SEC61p and SECYp is associated with ribosomes and nascent polypeptides during translocation, *Cell 71*, 489−503.
4. Hessa, T., Kim, H., Bihlmaier, K., Lundin, C., Boekel, J., Andersson, H., Nilsson, I., White, S. H., and von Heijne, G. (2005) Recognition of transmembrane helices by the endoplasmic reticulum translocon, *Nature 433*, 377−381.
5. Roosild, T. P., Greenwald, J., Vega, M., Castronovo, S., Riek, R., and Choe, S. (2005) NMR structure of Mistic, a membrane-integrating protein for membrane protein expression, *Science 307*, 1317−1321.
6. Tate, C. G. (2001) Overexpression of mammalian integral membrane proteins for structural studies, *FEBS. Lett. 504*, 94−98.
7. Garavito, R., and Ferguson-Miller, S. (2001) Detergents as tools in membrane biochemistry, *J. Biol. Chem. 276*, 32403−32406.
8. Ulmschneider, M. B., and Sansom, M. S. P. (2001) Amino acid distributions in integral membrane protein structures, *Biochim. Biophys. Acta 1512*, 1−14.
9. Cuthbertson, J. M., Doyle, D. A., and Sansom, M. S. P. (2005) Transmembrane helix prediction: a comparative evaluation and analysis, *Protein Eng. Des. Sel. 18*, 295−308.
10. Karplus, M. J., and McCammon, J. A. (2002) Molecular dynamics simulations of biomolecules, *Nat. Struct. Biol. 9*, 646−652.
11. Adcock, S. A., and McCammon, J. A. (2006) Molecular dynamics: survey of methods for simulating the activity of proteins, *Chem. Rev. 106*, 1589−1615.
12. Ash, W. L., Zlomislic, M. R., Oloo, E. O., and Tieleman, D. P. (2004) Computer simulations of membrane proteins, *Biochim. Biophys. Acta 1666*, 158−189.
13. Bond, P. J., and Sansom, M. S. P. (2003) Membrane protein dynamics vs. environment: simulations of OmpA in a micelle and in a bilayer, *J. Mol. Biol. 329*, 1035−1053.
14. Patargias, G., Bond, P. J., Deol, S. D., and Sansom, M. S. P. (2005) Molecular dynamics simulations of GlpF in a micelle vs. in a bilayer: conformational dynamics of a membrane protein as a function of environment, *J. Phys. Chem. B 109*, 575−582.
15. Bond, P. J., Cuthbertson, J. M., Deol, S. D., and Sansom, M. S. P. (2004) MD simulations of spontaneous membrane protein/detergent micelle formation, *J. Am. Chem. Soc. 126*, 15948−15949.
16. Braun, R., Engelman, D. M., and Schulten, K. (2004) Molecular dynamics simulations of micelle formation around dimeric Glycophorin A transmembrane helices, *Biophys. J. 87*, 754−763.
17. Lindahl, E., Hess, B., and van der Spoel, D. (2001) GROMACS 3.0: a package for molecular simulation and trajectory analysis, *J. Mol. Model. 7*, 306−317.
18. van Gunsteren, W. F., Kruger, P., Billeter, S. R., Mark, A. E., Eising, A. A., Scott, W. R. P., Huneberger, P. H., and Tironi, I. G. (1996) *Biomolecular Simulation: The GROMOS96 Manual and User Guide*, Biomos & Hochschulverlag AG an der ETH Zurich, Groningen & Zurich.
19. Hermans, J., Berendsen, H. J. C., van Gunsteren, W. F., and Postma, J. P. M. (1984) A consistent empirical potential for water−protein interactions, *Biopolymers 23*, 1513−1518.
20. Darden, T., York, D., and Pedersen, L. (1993) Particle mesh Ewald − an N.log(N) method for Ewald sums in large systems, *J. Chem. Phys. 98*, 10089−10092.
21. Essmann, U., Perera, L., Berkowitz, M. L., Darden, T., Lee, H., and Pedersen, L. G. (1995) A smooth particle mesh Ewald method, *J. Chem. Phys. 103*, 8577−8593.
22. Berendsen, H. J. C., Postma, J. P. M., van Gunsteren, W. F., DiNola, A., and Haak, J. R. (1984) Molecular dynamics with coupling to an external bath, *J. Chem. Phys. 81*, 3684−3690.
23. Hess, B., Bekker, H., Berendsen, H. J. C., and Fraaije, J. G. E. M. (1997) LINCS: A linear constraint solver for molecular simulations, *J. Comput. Chem. 18*, 1463−1472.
24. Kabsch, W., and Sander, C. (1983) Dictionary of protein secondary structure: pattern-recognition of hydrogen-bonded and geometrical features, *Biopolymers 22*, 2577−2637.
25. Humphrey, W., Dalke, A., and Schulten, K. (1996) VMD − Visual molecular dynamics, *J. Mol. Graph. 14*, 33−38.
26. Sanchez, R., and Sali, A. (2000) Comparative protein structure modeling. Introduction and practical examples with modeller, *Methods Mol. Biol. 143*, 97−129.
27. Li, H., Robertson, A. D., and Jensen, J. H. (2005) Very fast empirical prediction and interpretation of protein pK_a values, *Proteins: Struct., Funct., Bioinf. 61*, 704−721.
28. van Aalten, D. M., Bywater, R., Findlay, J. B., Hendlich, M., Hooft, R. W., and Vriend, G. (1996) PRODRG, a program for generating molecular topologies and unique molecular descriptors from coordinates of small molecules, *J. Comput.-Aided Mol. Des. 10*, 255−262.
29. Herrmann, K. W. (1966) Micellar properties of some zwitterionic surfactants, *J. Colloid Interface Sci. 22*, 352−359.
30. Tieleman, D. P., van der Spoel, D., and Berendsen, H. J. C. (2000) Molecular dynamics simulations of dodecylphosphocholine micelles at three different aggregate sizes: Micellar structure and chain relaxation, *J. Phys. Chem. B 104*, 6380−6388.
31. Bogusz, S., Venable, R. M., and Pastor, R. W. (2000) Molecular dynamics simulations of octyl glucoside micelles: Structural properties, *J. Phys. Chem. B 104*, 5462−5470.
32. Bogusz, S., Venable, R. M., and Pastor, R. W. (2001) Molecular dynamics simulations of octyl glucoside micelles: Dynamic properties, *J. Phys. Chem. B 105*, 8312−8321.
33. Braun, R., and Schulten, K. (2004) Molecular dynamics studies of sodium dodecyl sulfate aggregation about glycophorin-A transmembrane domain, *Biophys. J. 86*, 560A.
34. Böckmann, R. A., and Caflisch, A. (2005) Spontaneous formation of detergent micelles around the outer membrane protein OmpX, *Biophys. J. 86*, 3191−3204.
35. Li, J., Carroll, J., and Ellar, D. J. (1991) Crystal structure of insecticidal δ endotoxin from Bacillus thuringiensis at 2.5 Å resolution, *Nature 353*, 815−821.
36. Cramer, W. A., Heymann, J. B., Schendel, S. L., Deriy, B. N., Cohen, F. S., Elkins, P. A., and Stauffacher, C. V. (1995) Structure−function of the channel-forming colicins, *Annu. Rev. Biophys. Biomol. Struct. 24*, 611−641.
37. Lopez, C. F., Nielsen, S. O., Ensing, B., Moore, P. B., and Klein, M. L. (2005) Structure and dynamics of model pore insertion into a membrane, *Biophys. J. 88*, 3083−3094.
38. Bond, P. J., and Sansom, M. S. P. (2006) Insertion and assembly of membrane proteins via simulation, *J. Am. Chem. Soc. 128*, 2697−2704.
39. Kastenholz, M. A., and Hünenberger, P. H. (2004) Influence of artificial periodicity and ionic strength in molecular dynamics simulations of charged biomolecules employing lattice-sum methods, *J. Phys. Chem. B 108*, 774−788.
40. Beck, D. A. C., Armen, R. S., and Daggett, V. (2005) Cutoff size need not strongly influence molecular dynamics results for solvated polypeptides, *Biochemistry 44*, 609−616.

BI0608818